Forecasting Tropical Cyclone Recurvature. Part II: An Objective Technique Using an Empirical Orthogonal Function Representation of Vorticity Fields

DEBRA M. FORD,* RUSSELL L. ELSBERRY, PATRICK A. HARR, AND PAUL H. DOBOS

Department of Meteorology, Naval Postgraduate School, Monterey, California

(Manuscript received 9 March 1992, in final form 13 October 1992)

ABSTRACT

An empirical orthogonal function (EOF) representation of relative vorticity is used to forecast recurvature (change in storm heading from west through north to east of 360°) of western North Pacific tropical cyclones. A pattern recognition approach is adapted in which the synoptic conditions at recurvature time and each 12-h interval up to 96 h prior to recurvature are to be distinguished from the synoptic pattern for straight-mover storms. Synoptic descriptors are defined in terms of the time-dependent principal components of the vorticity fields for the individual maps. A standard discriminant analysis approach using 250-mb vorticity fields correctly identifies recurvers and straight movers in 80% and 66%, respectively, of the 782 cases. For a specific discriminant analysis that is derived to separate recurvers (74% correct) from straight movers (81% correct), the accuracy is higher than for the operational track prediction techniques and the official forecasts considered in Part I of this study. Although the accuracy of the discriminant analysis in identifying the time to recurvature in 12-h intervals is less than desired for operational use, this new technique has higher accuracy than the techniques evaluated in Part I. Better accuracy can be achieved if the time resolution requirements are relaxed, for example, into three groups (0–24 h, 36–72 h, and greater than 72 h until recurvature).

1. Introduction

As shown in Dobos and Elsberry (1993; Part I), the ability of three objective tropical cyclone track prediction aids and of the official Joint Typhoon Warning Center (JTWC) forecasts to predict recurvature is limited. Recurvature is defined as the change of direction from northwest through north to east of 360°, which typically occurs as the tropical cyclone passes through the subtropical ridge. As in Part I, the designation of recurvers and straight movers has been made by Miller et al. (1988), who also added a third category for erratic tracks that include a loop or a stair-step-type track. In this study, an objective technique for predicting the time to recurvature is developed and compared with the track prediction techniques evaluated in Part I.

As defined above, recurvature occurs as the tropical cyclone moves from the equatorward to the poleward side of the subtropical ridge. Prior to recurvature when the storm is equatorward of the subtropical ridge, the track and environmental conditions may be very similar to a straight mover (Fig. 1). However, progressive changes in the environmental flow then lead to departures of the recurver tracks from the straight movers.

The basic assumption in this study is that a particular synoptic pattern occurs during recurvature, and the antecedent conditions leading to the event should be accompanied by a progression of synoptic patterns that are distinguishable from straight-mover conditions. The recurvature sequence might be forecast using a pattern recognition approach if descriptors could be found that distinguish the synoptic patterns associated with recurving storms from conditions characterizing straight movers. Suppose two such synoptic descriptors existed (Fig. 2). If the set of environmental flow conditions that existed at recurvature time was unique from the synoptic conditions attending straight motion, the two clusters of points would be separated in this synoptic descriptor phase space. Furthermore, the set of conditions at intermediate times (e.g., 48 h in Fig. 2) prior to recurvature might also be characterized by separate clusters of points in such a hypothetical phase space. This scatter about the cluster means at intermediate times is expected because of the different rates at which recurvature occurs. Given a new case, its associated synoptic descriptors could be compared with the clusters in Fig. 2 to determine whether this situation is distinguishable as a recurver versus a straight mover, and perhaps even the most likely time to recurvature. No other potential predictors (e.g., latitude, longitude, storm size) will be included as the focus here is on the environmental conditions. A climatological study of

* Current affiliation: NOCC, COMNAVMARIANAS, Guam.

Corresponding author address: R. L. Elsberry, Code MR/Es, Department of Meteorology, Naval Postgraduate School, Monterey, CA 93943.

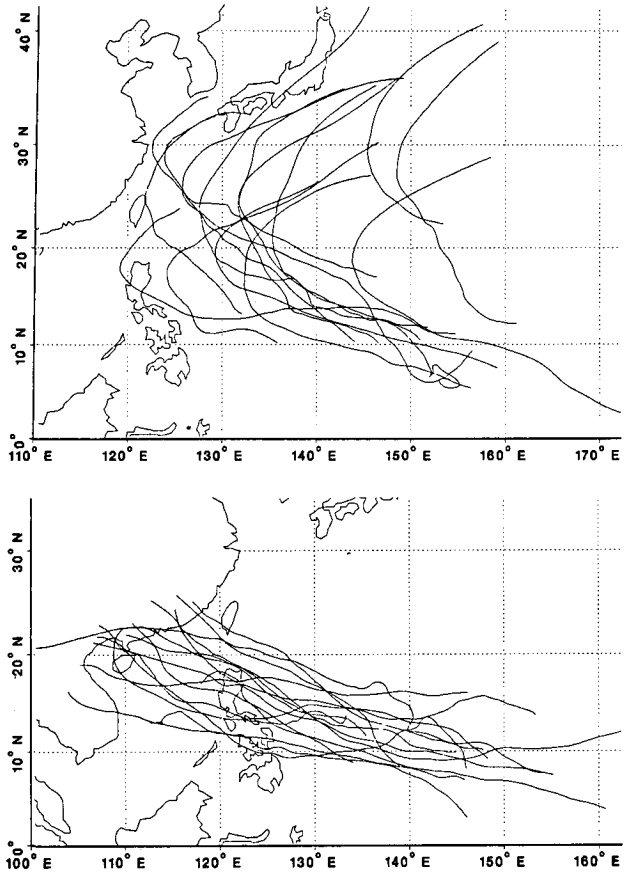

FIG. 1. Selected cases of recurvers (top), and straight movers (bottom) during 1979–84.

track types by Harr and Elsberry (1991) demonstrated that tropical cyclones forming in certain regions have a tendency toward recurving tracks, and storms in other locations may have either recurving or straight-moving tracks.

The objective of this paper is to search for synoptic descriptors as in the conceptual model in Fig. 2 to forecast the recurvature of tropical cyclones. In section 2, the synoptic descriptors will be defined as the time-dependent principal components of empirical orthogonal function (EOF) spatial patterns for the relative vorticity fields. The implicit assumptions here are that these vorticity fields will be well resolved from operational wind analyses, and the principal components will accurately represent the environmental flow conditions during recurvature. In section 3, a standard discriminant analysis will be applied in which the synoptic descriptors in Fig. 2 will be the canonical discriminant functions. The physical interpretation of the discriminant analysis approach used here is that the set of principal components that represent the environmental circulation at a specific time is to be classified into the group that has the most similar set of principal components as measured in multidimensional space. The discriminant analysis package objectively determines the combination of principal components that best separates the groups.

It will be shown that the synoptic patterns associated with recurvers can be distinguished from straight movers in about 75% of the situations. However, displays of the storm cases in the format of Fig. 2 will be used to illustrate rather clearly why little accuracy exists in estimating the time to recurvature in the critical 36–72-h interval. Nevertheless, the forecaster could use the knowledge that recurvature conditions are favored as part of the selection of the most likely track from among the objective track forecast aids. For example, an analog technique available at JTWC (Guam) has much improved accuracy when it is used selectively for only recurver cases or only straight-mover cases (T. Tsui 1990, personal communication). Consequently, the proposed pattern recognition approach may help improve tropical cyclone track forecasting.

2. Data and approach

a. Storm tracks

Because of the requirement in Part I to form a homogeneous sample in the forecast technique evaluations, the western North Pacific cases during 1979–84 in Part I are a subset of the potential sample of cases. In addition to the geographical domain and storm intensity criteria in Part I, the only other requirement here was the availability of an analysis of the meridional and zonal wind components at 700, 400, and 250 mb.

As in Part I, identification of the storms as recurvers or straight movers is based on the tropical cyclone track categories assigned by Miller et al. (1988). None of the cases identified as odd movers by Miller et al. are used since a definite classification is required to develop the objective technique. For each recurving tropical cyclone, the storm heading between successive 6-h JTWC best-track positions is computed and the recurvature time is identified as either the 0000 or 1200 UTC nearest the time when the storm heading changed

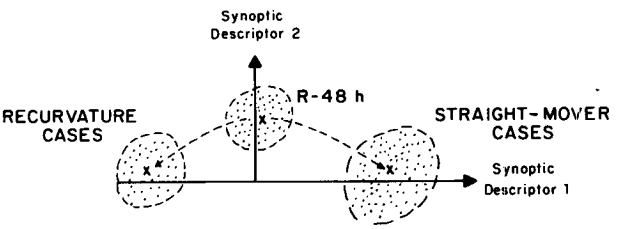

FIG. 2. Conceptual model of clusters of recurvature cases, straight-mover cases, and cases at 48 h prior to recurvature (*R*-48h) in a hypothetical two-dimensional synoptic descriptor space in which the first two descriptors are orthogonal. Progression from the straight-mover cluster through *R*-48h to recurvature is implied by the cluster arrangement.

from west of 360° to east of 360°. Synoptic map times prior to recurvature will be referred to as *R-XXh*, where *R* denotes recurvature and *XXh* indicates the number of hours. Recurver cases within 96 h of recurvature are then categorized based on time to recurvature as *R*-96h through *R*-00h. Cases more than 96 h prior to recurvature are identified as prerecurvers (PR).

The straight-mover cases are identified as nonrecurvers (NR) if a minimum of 72 h remains in the track to establish that recurvature did not occur. This 72-h interval is selected to be consistent with the forecast interval in the JTWC warnings. The portion of the recurver's track more than 96 h prior to recurvature (PR) will be assumed to be similar to the NR tracks (see discussion of Fig. 3). A final verification set, which includes the recurver set at all times prior to recurvature and the straight-mover cases at least 72 h prior to the last position, contains 782 out of an original sample of 1573 cases.

b. *Vorticity field representation*

Tropical cyclone motion can be described in terms of vorticity dynamics (e.g., Elsberry 1987). Thus, the synoptic patterns around the tropical cyclone will be described in terms of the vorticity fields derived from operationally analyzed winds. These global band analysis (GBA) wind fields were generated every 12 h by the United States Navy Fleet Numerical Oceanography Center. The GBA has a global longitudinal coverage between 40.956°S and 59.745°N. The analyses are on a Mercator grid with spacing of 2.5° latitude at 22.5°N and 22.5°S. Analyses are based on surface observations, ship reports, rawinsondes, pibals, aircraft reports, and satellite-derived cloud-motion vectors. When a tropical cyclone is present, eight bogus winds are inserted at the surface very near (80 km or 43 n mi) the center of the cyclone, and are coupled vertically via the thermal wind equation using temperature analyses at the intermediate levels. A detailed description of the GBA is contained in the U.S. Naval Weather Service (1975) manual.

A linear interpolation scheme is used to interpolate the GBA zonal and meridional wind components onto a storm-centered grid that has a fixed zonal and meridional separation of 277.8 km (150 n mi). The grid is geographically oriented with 31 grid points west to east and 17 grid points south to north. The center of the cyclone (the JTWC warning position) is always located at grid point (16, 9). The relative vorticity is calculated using centered finite differences at the internal grid points, and one-sided differences at the grid boundaries.

c. *EOF analysis*

Empirical orthogonal functions (EOF) will be used as the synoptic descriptors of the relative vorticity fields as proposed in Fig. 2. In EOF analysis, the structure of the geophysical data determines the spatial dependence of the functions. After the spatial patterns (eigenvectors) have been calculated, the contribution of each of these modes to the total field is represented by the EOF coefficients (principal components). These coefficients will be used to represent the time dependence in the vorticity fields as in Fig. 2. A comprehensive description of the EOF technique is given in Preisendorfer et al. (1981).

EOF predictors have been used successfully in statistical synoptic models to forecast tropical cyclone motion and intensity changes (Shaffer and Elsberry 1982; Peak et al. 1986; Schott et al. 1987; Elsberry et al. 1988). These studies verify that the EOF coefficients represent the time dependence in the environmental fields around tropical cyclones. Sparse or erroneous observations will lead to inaccuracies in the synoptic representation. However, the large-scale vorticity features represented by the EOF technique are less likely to be affected than individual grid points used in other statistical techniques. Because relatively few EOF coefficients are required to represent most of the variance in the synoptic patterns, the EOF technique is more efficient than the use of every grid point in the field.

The EOF method applied to the relative vorticity fields at 700, 400, and 250 mb (Gunzelman 1991) is identical to the procedures described by Peak et al. (1986) and Elsberry et al. (1988). The EOF analysis is based on a dependent sample of 682 cases during 1979–83 that Peak et al. (1986) also used. In this application, $X(527)$ eigenvectors are calculated from a normalized $XY(527 \times 682)$ matrix of $X(527)$ gridpoint values for the $Y(682)$ cases. The first eigenvector (spatial pattern) contains the largest variance. The second eigenvector contains the largest amount of the variance not explained by the first, and so on. Once the eigenvectors are determined from the dependent dataset, the time dependence in the synoptic pattern for each case is contained in the EOF coefficients (principal components). A negative EOF coefficient indicates that the identical spatial pattern applies, except that the maxima and minima are reversed. The original gridpoint values can be recovered by the linear summation of the products of the eigenvectors and their associated coefficients.

The Preisendorfer and Barnett (1977) Monte Carlo technique may be used to distinguish between eigenvectors with signal versus those with noise. In this method, EOF coefficients for the physical data are compared to EOF coefficients for randomly generated data. If the physical EOF coefficient deviates more than two standard deviations from the EOF coefficient computed from a random vorticity field, there is reasonable assurance that the associated eigenvector is describing signal rather than noise. Based on this method, the first 45 EOF modes are retained as potential descriptors of the synoptic fields associated with recurvature. The first 45 modes explain 72.8%, 76.9%, and

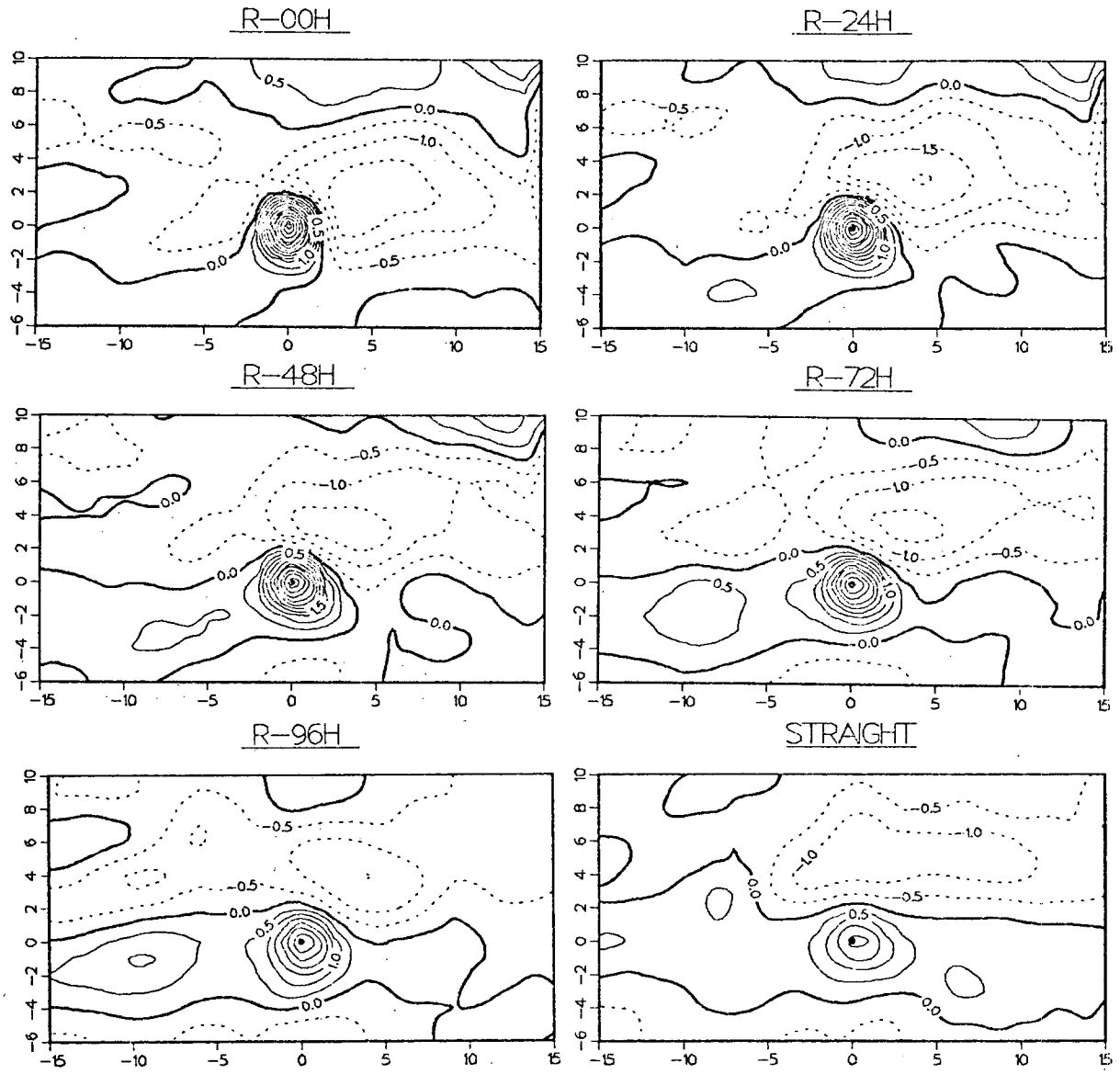

FIG. 3. Relative vorticity (10^{-5} s^{-1}, positive values are solid) at 700 mb reconstructed from the mean of the first 45 EOF modes for the set of recurving storms at *R*-00h (top left), *R*-24h (top right), *R*-48h (middle left), *R*-72h (middle right), *R*-96h (bottom left), and for the nonrecurving storms (bottom right). The storm center (black dot) is always at the same position on the 31 × 17 grid.

77.5% of the variances in the vorticities at 700, 400, and 250 mb, respectively.

Vorticity fields for the sets of recurvers and straight movers shown in Fig. 1 are reconstructed from the 45 mean EOF coefficients for each time-to-recurvature group to illustrate the sequence of the synoptic patterns associated with recurvature. Because similar patterns are found at 400 and 250 mb, only the 700-mb pattern (Fig. 3) will be discussed. The sequence starts with the straight-mover pattern in which the subtropical ridge is well defined by the broad anticyclonic (negative) vorticity center to the north of the cyclone center. Such a pattern would be expected to produce westerly or northwesterly storm motion and a straight-type track. At *R*-96h, the anticyclonic vorticity associated with the subtropical ridge is weaker to the north and stronger to the northeast of the storm center than it was in the NR pattern. Proceeding toward recurvature time, the cyclonic (positive) vorticity associated with the storm and the anticyclonic vorticity associated with the subtropical ridge increase in magnitude as the composite recurver moves north-northwest around the ridge. At recurvature time, the storm center position is at the axis of the ridge and only a relatively weak region of

anticyclonic vorticity is found between the storm and the midlatitude cyclonic vorticity to the north. Thus, the sets of mean EOF coefficients define a physically realistic description of the environmental fields as the tropical cyclone changes from a straight mover to a recurver.

To illustrate the potential for using EOF coefficients as in the conceptual model in Fig. 2, univariate statistics for EOF mode 1 coefficients at 250 mb are compared in Fig. 4. Mode 1 not only accounts for the largest percent of the variance in the synoptic vorticity patterns, it is also selected as the first predictor in the discriminant analysis discussed below. The EOF mode 1 group means vary almost linearly from large negative values at recurvature to near-zero values at 36 h. A curvilinear relationship exists among the group means between 48 h and the other times through the nonrecurvers (NR). Variances are large and the considerable overlap among groups indicates the variability in vorticity patterns that lead to recurvature. The similar group means for NR, PR, *R*-96h, and *R*-84h times make it unlikely that the discriminant analysis could consistently separate these groups based on mode 1 only.

3. Discriminant analysis

A standard discriminant analysis technique (Dixon 1988) is used to select the EOF predictors for forecasting tropical cyclone recurvature. A linear combination of predictors called a canonical discriminant function is formed that provides the best separation among the groups. Second and subsequent canonical discriminant functions are then formed that are orthogonal and best separate the groups on the basis of associations not used in the preceding canonical discriminant functions. The maximum number of canonical discriminant functions is equal to the number of groups minus one or the number of predictor variables, whichever is less. Consequently, the synoptic descriptions of the conceptual model in Fig. 2 become

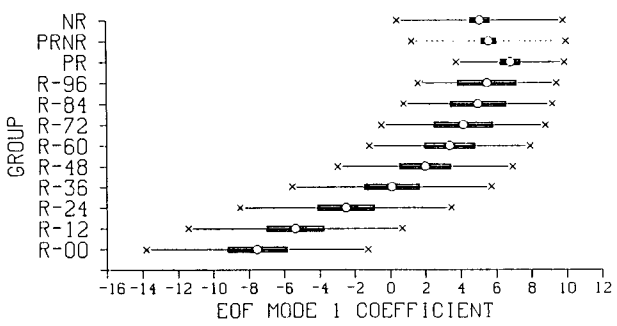

FIG. 4. Univariate statistics of EOF mode 1 for the 250-mb vorticity fields. Means (open circle), 95% confidence intervals (solid bar), and standard deviations (×) for time-to-recurvature groups and the combined prerecurver (PR) and nonrecurver (NR) groups.

these canonical discriminant functions in this approach.

Although discriminant analysis provides an objective approach to predictor selection, the user must still make many choices both in its application and evaluation. Searching for the optimum discriminant analysis model requires extensive testing and should be conducted on a large sample population. Consequently, the discriminant analysis model will be developed with the entire sample, which means that no cases will be available for an independent verification set. The discriminant analysis package includes a jackknife option that indicates the accuracy to be expected with independent testing. In this procedure, one of the 782 cases is withheld and the remaining cases are used to derive the analysis model, which is then tested on the withheld case. This process is repeated 782 times and the summary of the individual cases is the jackknifed result.

a. Selection of predictors

The discriminant analysis approach provides a completely objective and statistically based method of selecting the predictors. Potential predictors are selected from the first 45 EOF coefficients representing the 250-mb vorticity fields. This level produced slightly better forecasts than the 700- or 400-mb levels in a test (not shown) with a similar analysis approach. Although all 45 EOF coefficients could be used, the objective is to obtain the best classification accuracy with the fewest possible predictors. Such an efficient solution is sought by performing ten stepwise discriminant analyses (Table 1). The first analysis is restricted to one mode, the second is restricted to two modes, and so on until ten modes are selected in the tenth analysis model. Limits are relaxed in the discriminant analysis procedure to ensure the selection of up to ten predictors. Nevertheless, subsequent statistical tests for the analyses in Table 1 indicate that each of the selected modes is significant to the separation of recurver groups at the 0.01 level or better.

An optimal forecast model is selected from Table 1 by examining gains in forecast accuracy (see the percent correct and penalty *R*-score definitions in Part I) as the number of modes in the analysis is increased from one to ten. As expected, the jackknifed results in columns 5–8 have smaller accuracies than the dependent results in columns 1–5. The general trend is toward smaller penalty *R* scores and higher percent-correct classifications as the number of modes increases from one to ten.

The seven-mode discriminant analysis model in Table 1 is considered to be the best because the addition of mode 24 as the seventh mode improves all measures of classification accuracy relative to the accuracy for the models with six or fewer modes. However, the addition of mode 45 as the eighth mode results in deg-

TABLE 1. Penalty R score (see Part I for definition) and percent correctly classified in recurvers (R-00h to R-72h) or straight movers (R-84h to PRNR) for a sequence of discriminant analyses in which the number of modes is increased by one. Jackknifed results from successively withholding one case from the sample indicate the accuracy expected with independent testing. The percent of recurvers (%R), straight movers (%S), and total (%T) sample correctly classified along with the penalty R score are defined in Part I.

Dependent sample				Jackknifed results				Modes									
R score	%R	%S	%T	R score	%R	%S	%T										
2.24	77	66	71	2.24	77	66	71	1									
2.23	74	69	71	2.25	74	69	71	1	2								
2.01	78	70	73	2.06	77	70	73	1	2	3							
2.02	75	69	72	2.07	75	69	71	1	2	3	4						
1.95	77	67	71	2.04	76	67	71	1	2	3	4	5					
1.91	77	64	70	1.98	76	64	69	1	2	3	4	5	6				
1.88	80	66	72	2.00	79	64	69	1	2	3	4	5	6	24			
1.95	77	66	71	2.09	76	64	69	1	2	3	4	5	6	24	45		
1.89	78	67	72	2.00	77	66	71	1	2	3	4	5	6	24	45	9	
1.87	77	69	72	2.08	75	68	71	1	2	3	4	5	6	24	45	9	14

radation in both measures of accuracy, and mode 45 is on the margin between signal- and noise-containing modes. The addition of mode 9 in the nine-mode model produces only a slight improvement over the eight-mode analysis and only results in accuracies nearly equal to those for the seven-mode analysis. Some improvement is again noted by the addition of a tenth predictor, but the recurver %R(77) is less than the %R(80) for the seven-mode model. Although the seven modes in Table 1 may be combined in an optimum manner to discriminate among the nine categories of recurvature plus nonrecurvers, these seven modes are not necessarily the best combination to reconstruct the relative vorticity field as in Fig. 3.

The forecast-versus-observed matrix for the seven-mode discriminant analysis model is presented in Table 2. The format of this table is similar to those presented in Part I for three objective techniques and the official warnings. Classification into 12-h categories is most accurate near recurvature (R-00h = 60%, R-12h = 29%, and R-24h = 29%), and in the straight-track categories (R-96h = 29% and the combination of prerecurvers (PR) and nonrecurvers (NR) = 47%). Accuracies in the intermediate categories only range from 7% to 22%.

Bar charts (Fig. 5) of the percent of the observed cases in each 12-h time-to-recurvature category that are forecast into each group illustrate the relatively poor ability of the model to pinpoint the time to recurvature among the R-36h through R-84h cases. The intermediate 12-h categories not shown in Fig. 5 tend to have characteristics intermediate to the 24-h bar charts. Cases belonging to the R-00h, R-24h, R-96h, and PRNR groups are more frequently correctly classified or classified within one to two 12-h categories of the correct time than those belonging to the R-48h and R-72h groups. The R-36h (not shown), and to a lesser extent the R-48h through R-72h cases, are classified into all groups with nearly the same frequency, which reflects little ability to correctly distinguish the time to recurvature for these synoptic situations. However, only 28% of the R-48h cases were misclassified into straight-track groups.

TABLE 2. Observed versus forecast matrix for the verification set using the seven-mode discriminant analysis model at 250 mb, and the percent correctly classified into specific 12-h categories prior to recurvature time. The overall percent correct for recurvers (R-00h to R-72h) is 268 of 337 cases or 80%, for straight movers is 294 of 445 cases or 66%, and for the combined sample is 562 of 782 cases or 72%.

		Forecast										
		00	12	24	36	48	60	72	84	96	PRNR	Percentage
Observed	R-00h	33	12	2	2	1	0	1	3	0	1	60
	R-12h	17	16	10	4	3	0	1	1	2	2	29
	R-24h	5	13	16	4	6	3	0	3	2	3	29
	R-36h	2	8	9	6	7	3	2	6	4	5	12
	R-48h	1	3	6	7	6	7	3	1	7	5	13
	R-60h	2	0	1	9	3	9	6	2	3	6	22
	R-72h	0	2	1	2	3	5	6	4	3	6	19
	R-84h	0	0	2	1	2	6	2	2	6	9	7
	R-96h	0	0	0	3	1	5	0	3	7	5	29
	PRNR	2	5	16	22	31	32	21	25	53	184	47

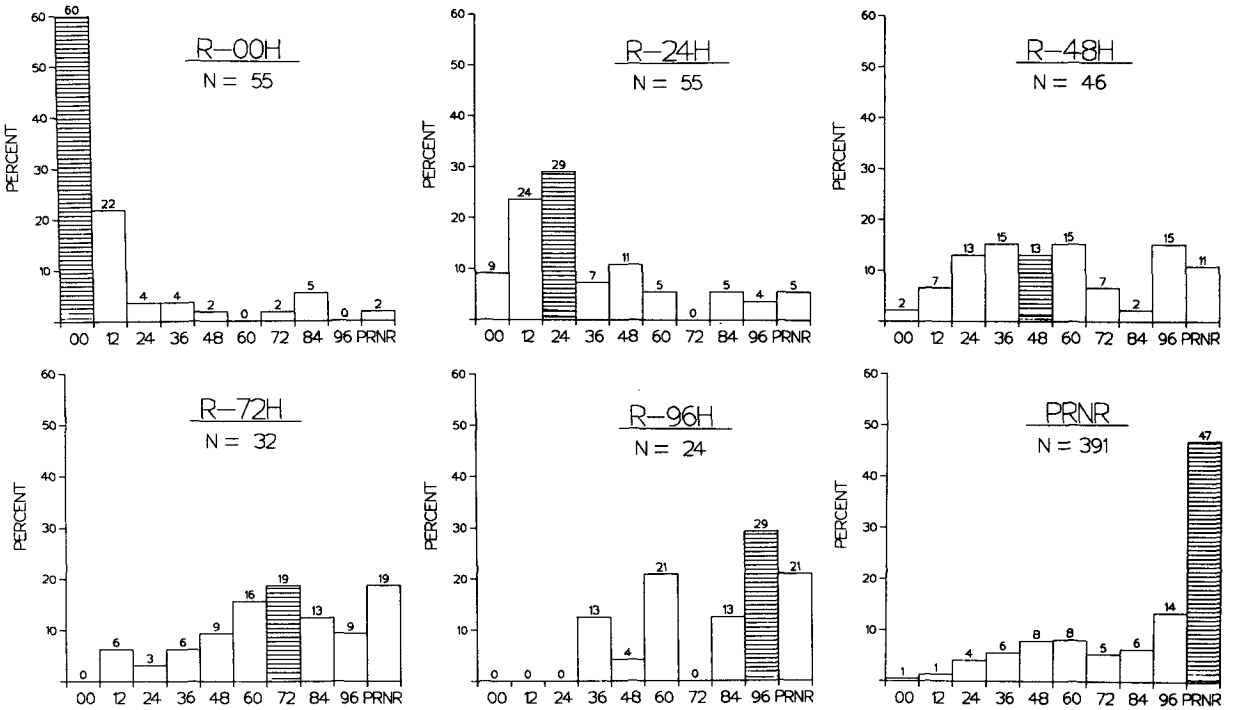

FIG. 5. Percent classifications by the seven-mode discriminant analysis at 250 mb into various 12-h time-to-recurvature groups for cases verifying at *R*-00h (top left), *R*-24h (top middle), *R*-48h (top right), *R*-72h (bottom left), *R*-96h (bottom middle), and PRNR (bottom right). Shaded bars indicate the percent in the correctly classified category.

In the two-category classification, differentiation of a recurver within 72 h of actual recurvature from a straight mover is considered successful for forecasts in the upper-left group (268) in Table 2 versus in the upper right (69). That is, the model correctly identifies synoptic situations that will lead to recurvature within the 72-h forecast period with 80% accuracy. Similarly, identification of a storm as a straight mover (more than 72 h from recurvature or PRNR) occurs if the forecast is in the lower-right group (294) rather than in the lower-left group (151). That is, the accuracy for straight-track situations is only 66%, so the combined accuracy in predicting track type is 72%. An almost homogeneous comparison with the 782 forecasts in Table 2 can be made for the subset of 730 cases for which a climatology and persistence (CLIPER) forecast could be generated (omits 52 cases lacking the past 12- or 24-h position required in CLIPER). The corresponding $\%R$, $\%S$, and $\%T$ for CLIPER are 62%, 85%, and 75%, which are similar values to the 53%, 86%, and 74% for a sample of 366 CLIPER forecasts in Part I. Given the 18% difference in percent correct and sample sizes exceeding 700 cases, it is highly likely that the discriminant analysis technique has skill relative to CLIPER for distinguishing recurvers. By contrast, the discriminant analysis technique is not skillful relative to CLIPER in distinguishing straight movers. Whereas the discriminant analysis technique overpredicts recurvature situations (too many forecasts in the lower-left group in Table 2), the CLIPER has a bias toward predicting straight movers (see Part I). Because more straight movers (445) than recurvers (337) occur in Table 2, the overall percent correct for the discriminant analysis technique (72%) is less than for CLIPER (75%). However, it is emphasized that the important forecast decision is to detect recurvature, and the discriminant analysis technique appears to have skill relative to CLIPER in these situations.

The most skillful objective technique in a homogeneous (but much smaller) sample comparison in Part I was the one-way influence tropical cyclone model (OTCM). Only 446 of the 782 discriminant analysis cases in Table 2 had a corresponding OTCM forecast. The $\%R$, $\%S$, and $\%T$ for this OTCM sample are 61%, 81%, and 73%, respectively (values of 62%, 80%, and 73% were found in Part I). As was the case for CLIPER, the discriminant analysis technique appears to be more accurate for recurvers, less accurate for straight movers, and also less accurate in terms of overall percent correct. The same conclusion holds for the subset of 633 JTWC forecasts for which the corresponding $\%R$, $\%S$, and $\%T$ are 58%, 82%, and 73% respectively (values of 56%, 84%, and 73% in Part I). Notice that these nonhomogeneous samples have the same relative accuracies among CLIPER, OTCM, and JTWC as in the homogeneous comparison in Part I. Given the apparent

TABLE 3. Observed versus forecast matrix for the verification set using a specific discriminant analysis model at 250 mb to distinguish only the two categories of recurvers (*R*-00h to *R*-72h) and straight movers (*R*-84h to PRNR). The percent correctly classified into specific categories prior to recurvature time is also given for comparison with Table 2. The overall percent correct for recurvers is 74%, for straight movers is 81%, and for the combined sample is 78%.

		Forecast		
		Recurver	Straight	Percentage
Observed	*R*-00h	53	2	96
	R-12h	52	4	93
	R-24h	46	9	84
	R-36h	37	15	71
	R-48h	27	19	59
	R-60h	23	18	56
	R-72h	10	22	31
	R-84h	6	24	80
	R-96h	6	18	75
	PRNR	73	318	81

skill (18% improvement) relative to CLIPER in a sample exceeding 700 cases, a conclusion that the discriminant analysis technique has merit seems justifiable.

b. Alternate forecast intervals

If the only requirement is to distinguish recurvers from straight movers, a two-category discriminant analysis model may be derived (Table 3). For the same sample as in Table 2, the $\%R$, $\%S$, and $\%T$ for the two-category analysis are 74%, 81%, and 78%. Although some degradation (6%) is noted in distinguishing recurvers, the capability to isolate straight-mover cases is greatly improved (15%), so that the $\%T$ value indicates a higher accuracy than the objective track techniques (largest value of 75%). The verifications within each 12-h category in Table 3 have highly variable accuracies. The percent correctly classified decreases from 96% for cases at recurvature time to 31% at *R*-72h. This is because times closer to recurvature are more distinct from the straight-mover group and are therefore more readily recognized as recurvers.

A more useful distinction to the forecaster would be separation into imminent, medium, and small likelihood of recurvature (Table 4). As in Part I, the imminent group is defined as the *R*-00h to *R*-24h cases, the medium group as all *R*-36h to *R*-72h cases, and the small group as the *R*-84h through PRNR cases. Discriminant analysis correctly classifies the sample into imminent, medium, or small categories with 73%, 50%, and 68% accuracy, respectively. While this three-group classifications scheme increases the time resolution in the recurvature prediction, the overall ability to correctly classify track types during the 72-h forecast period is 73% versus 78% for the two-group analysis. Although accuracy of the three-group scheme in identifying straight-moving situations is degraded to 68%, the accuracy in distinguishing recurvers is increased to 79%. Introduction of the medium group thus has increased the separation among the 12-h data categories in the imminent recurver group and the nonrecurver categories.

Discriminant analysis into the ten 12-h time-to-recurvature groups *R*-00h to *R*-96h plus PRNR (Table 2) maximizes the time resolution of the predictions for this dataset, but at the expense of forecast accuracy. For example, the overall ability to distinguish between recurver and straight-track situations is 72% as compared to the 78% and 73% accuracy achieved by the two-group (Table 3) and the three-group (Table 4) models, respectively. The ability of the ten-group analysis to discern imminent, medium, and small likelihood of recurvature is generally 2%–6% less than for the three-group model. As expected, accuracy within each 12-h time-to-recurvature category is considerably less than for the broader imminent–medium–small or recurver–straight categories.

Plotting the time-group centroids in terms of the canonical discriminant functions (Figs. 6, 7, and 8) provides a graphic representation of the ability of the two-, three-, and ten-group discriminant analysis models to separate the cases. These group centroids are the mean values for all cases in the time group. The distances between these time centroids are indicative of the relative separations achieved by each of the three discriminant analysis models, and thus provide an illustration along the lines of the conceptual model in Fig. 2. Although the scatter about these mean values is not shown, it may be similar to that in Fig. 4 since the discriminant functions are weighted combinations of such principal components. In particular, an overlap

TABLE 4. Observed versus forecast matrix for the verification set using the discriminant analysis model at 250 mb for the three categories of imminent (*R*-00h to *R*-24h), medium (*R*-36h to *R*-72h), and small (*R*-84 to PRNR). The percent correctly classified into specific categories prior to recurvature time is also given for comparison with Table 2. The overall percent correct for imminent, medium, and small categories are 73%, 50%, and 68%, respectively. The overall percent correct in the recurver (*R*-00h to *R*-72h) and straight-mover (*R*-84h through PRNR) groups are 79% and 68%, respectively.

		Forecast			
		Imminent	Medium	Small	Percentage
Observed	*R*-00h	46	5	4	84
	R-12h	44	7	5	78
	R-24h	31	16	8	56
	R-36h	18	19	15	45
	R-48h	8	25	13	54
	R-60h	3	25	13	61
	R-72h	3	16	13	50
	R-84h	2	13	15	50
	R-96h	0	10	14	58
	PRNR	22	97	272	70

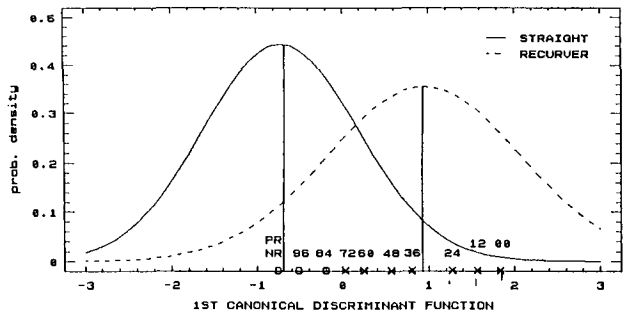

FIG. 6. Group centroids (vertical lines) and fitted distributions of the straight-movers (solid) and recurvers (dashed) cases along the first (only) canonical discriminant function axis for the two-group model. Time centroids for the PRNR through *R*-00h in 12-h intervals are indicated along the axis for straight movers (○) and recurvers (×).

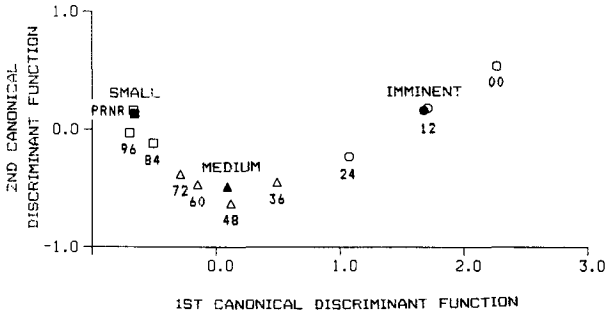

FIG. 7. Group centroids (solid markers) and 12-h time centroids (open markers) in the two canonical discriminant functions of the three-group model. The three groups are imminent (circles), medium (triangles), and small (squares) likelihood of recurvature.

between adjacent clusters leads to the uncertainty in resolving cases into discrete categories.

Since the number of canonical discriminant functions is one less than the number of groups, a one-dimensional plot is presented for the two-group model (Fig. 6). In this case, the discriminant function is a weighted combination of six EOF coefficients. The time centroids of the *R*-84h through PRNR categories that comprise the straight-track group are all closer to the straight-group centroid than to the recurver-group centroid. However, the *R*-72h (which belongs in the recurver group) centroid is slightly closer to the straight-group centroid. While the actual distribution of individual cases determines the model accuracy reported in Table 3, the relative positions of the time centroids in Fig. 6 illustrate why the two-group model is better at correctly classifying straight-track cases (81%) than it is at correctly identifying recurver cases (74%). The fitted distributions of the straight-mover cases are more closely distributed about their group centroid than are the cases in the recurver group. Within the area of overlap between the two distributions, a large number of the recurver cases may be misclassified by the two-group model.

As in the conceptual model in Fig. 2, the three-group and ten-group model centroids (Figs. 7 and 8) are spatially separated in a curvilinear fashion that reflects a consistent time trend in the group centroids. These distributions illustrate why the forecast accuracy is higher for the *R*-00h or the PRNR groups. A normal distribution of cases for each time group would result in an ellipsoidal pattern centered on each of these centroids. A case in an intermediate time group such as *R*-48h has neighboring groups on either side that may be misclassified. By contrast, *R*-00h or PRNR groups have no neighboring group on one side that would result in erroneous classifications. For both the three- and ten-group models (Tables 4 and 2), forecast accuracy is notably higher in the end groups. The success of the three-group model is illustrated in Fig. 7 by the clustering of the time-to-recurvature centroids about the appropriate group mean. Notice that the 72-h centroid is clearly closer to the medium group centroid than to the small likelihood of recurvature group centroid, unlike in Fig. 6.

A proper geometric representation of the ten-group discriminant analysis model would require a 9D plot. With the 2D plot of the first and second discriminant functions (Fig. 8), differences in forecast skill for the ten-group model are more difficult to interpret. In general, the better-separated groups in Fig. 8 demonstrate better classification accuracy. For example, the *R*-00h to *R*-24h centroids are better separated than those for *R*-36h through *R*-96h. The scatter among cases in the 48-h and 72-h groups in Fig. 5 indicates an overlap with the full range of group centroid means.

Ultimately, the number of time-to-recurvature categories must be a trade-off between the forecaster's need to specify a precise time of recurvature versus diminishing accuracy as more precision is attempted. As indicated in Figs. 6–8, the decreasing separations among the group means, and the increasing overlap among the cases belonging to individual time-to-recurvature groups, will limit ability to accurately forecast the time to recurvature.

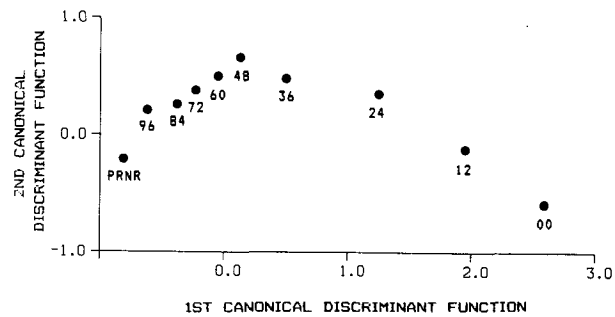

FIG. 8. Group (and time) centroids in 12-h intervals in terms of the first two of the nine canonical discriminant functions for the ten-group model.

4. Forecast examples

Operational application of a discriminant analysis model using EOF predictors to forecast tropical cyclone recurvature is relatively simple. Only a microcomputer would be required to interpolate the analyzed wind fields onto the storm-centered grid, compute the vorticity at the grid points, calculate the EOF coefficients corresponding to the vorticity field, and solve for the discriminant functions for each of the time-to-recurvature groups. The forecast would be the group that has the largest discriminant function.

In this section, forecast examples are presented for a recurver (Supertyphoon Vanessa), a straight mover (Typhoon Agnes), and an odd mover (Supertyphoon Bill). Although these cases are from the dependent sample, the forecast accuracy for these three storms is typical of other storms in the dataset.

The discriminant analysis forecasts of the time to recurvature for Supertyphoon Vanessa are shown in Fig. 9. Supertyphoon Vanessa tracked along the southern side of the subtropical ridge for nearly five days before sharply recurving (ATCR 1984). Only the two discriminant analysis model forecasts of *R*-72h for times greater than 96 h before recurvature (PR) are clearly erroneous. All forecasts within 72 h of recurvature are correct predictions of a recurver-type track. Although only three of the seven recurver-type track forecasts are exactly correct (*R*-00h, *R*-48h, and *R*-72h), the forecasts tend to progress in a sequential manner toward recurvature (*R*-72h, *R*-72h, *R*-48h, *R*-48h, *R*-36h, *R*-36h, *R*-00h). The rapid rate of recurvature in this case was not predicted in advance since the value changed abruptly from *R*-36h to *R*-00h only as recurvature occurred. The 12-h forecast sequences for most of the recurving storms in the sample have a similar progression. Such a consistent trend toward recurvature in successive operational forecasts would add confidence to the individual 12-h recurving-track forecasts.

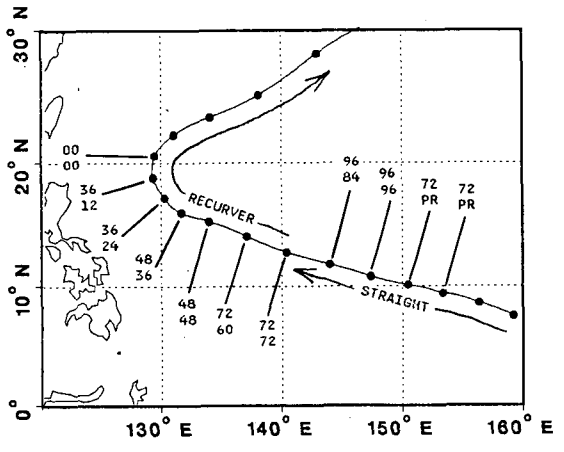

FIG. 9. Time to recurvature (bottom number) and forecast time (upper number) in 12-h increments for Supertyphoon Vanessa during 22–31 October 1984 (dots). Straight-moving (greater than 72 h to recurvature) and recurver (within *R*-72h) stages are indicated along the track.

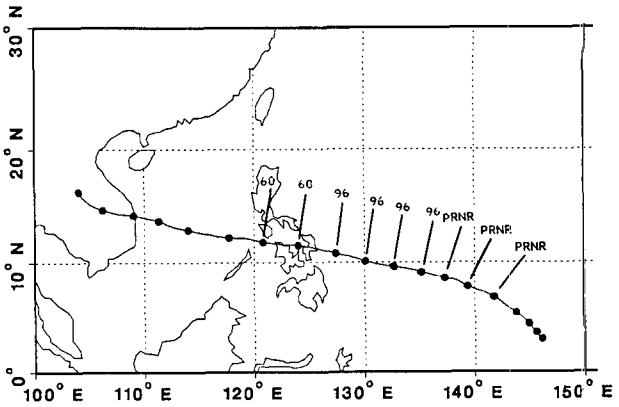

FIG. 10. Forecasts of prerecurvature (PR) or nonrecurvature (NR) or the time to recurvature in 12-h increments for Typhoon Agnes during 1–8 November 1984 (dots).

The discriminant analysis model forecasts for Typhoon Agnes are presented in Fig. 10. Typhoon Agnes tracked west-northwest under the influence of an easterly steering flow along the south side of a deep mid- to low-level subtropical ridge that extended from the date line west to the coast of Vietnam (ATCR 1984). Seven of the nine forecasts correctly predicted straight-track motion during the 72-h forecast period. The last two forecasts of recurvature in 60 h are mispredictions of the track type, since Agnes continued westward for at least 60 h until landfall in Vietnam and subsequent dissipation.

The forecast model in this study was not designed to distinguish odd-mover behavior such as loops and stair-step tracks. Therefore, forecasts based on the vorticity fields preceding or during erratic motion cannot provide accurate information on the storm track. However, the discriminant analysis may indicate whether the next segment of the track fits either of the straight or recurver track categories.

The time-to-recurvature forecasts for Supertyphoon Bill, classified as an odd mover, are shown in Fig. 11. The model correctly identifies the straight-track segment in the early forecasts. As Bill began to recurve around the western end of the subtropical ridge, the midlatitude trough passed to the north and weakened the ridge, which slowed Bill's progress. The intense low-level circulation in the Philippine Sea associated with Typhoon Clara, and the strengthening northeast monsoon flow, forced Bill to the southeast in an anticyclonic loop, causing the storm to weaken rapidly (ATCR 1984). This set of discriminant analysis forecasts is unusual in that a sudden transition occurs from straight-track predictions (*R*-96h) to the recurver predictions (*R*-24h, *R*-12h, and *R*-00h). The model fore-

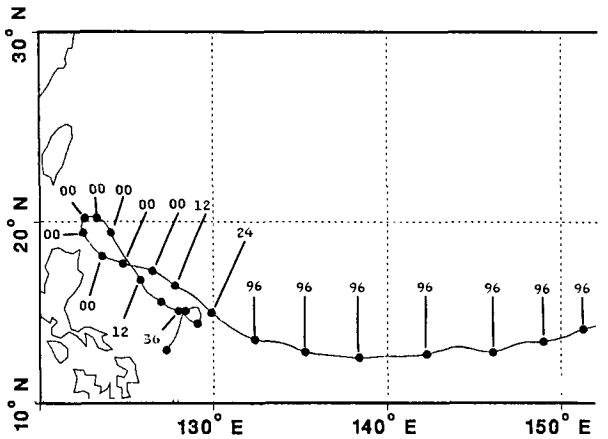

FIG. 11. As in Fig. 10 except for Supertyphoon Bill during 8–21 November 1984 in 12-h intervals (dots).

casts for recurving storms tend to transition more appropriately through successive recurvature classification categories. Although the forecaster would probably have recognized the binary interaction with Clara, a straightforward application of the discriminant analysis predictions during this period would obviously be misleading.

5. Conclusions

The feasibility of using an EOF representation to identify the vorticity patterns associated with tropical cyclone recurvature has been demonstrated. In this approach, relative vorticity fields are represented by 45 orthogonal eigenvectors that represent spatial patterns and account for 73%–78% of the variance.

As suggested by the conceptual model in Fig. 2, the first goal of a pattern recognition model is to distinguish between straight and recurving tropical cyclone motion during the 72-h forecast period. A second goal is to forecast the time to recurvature with 12-h accuracy.

Using a standard discriminant analysis package provides linear combinations of the EOF coefficients into discriminant functions that are the synoptic descriptors in Fig. 2. The entire set of 782 cases from 97 recurving and straight-moving tropical cyclones is used to both derive and test the model. Based on a large (but not homogeneous) sample, a discriminant analysis model at 250 mb appears to have skill relative to CLIPER (see Part I) in identifying recurvers (80%), but does not have skill for straight (66%) motion. The accuracy in distinguishing among the specific 12-h time-to-recurvature group (*R*-00h through *R*-96h) plus the combined straight mover and recurving storm cases more than 96 h prior to recurvature (PRNR) is only 60%, 29%, 29%, 12%, 13%, 22%, 19%, 7%, 29%, and 47%, respectively. Although the accuracy in identifying the time to recurvature is less than desired for operational use, these values show skill relative to CLIPER and the official JTWC forecasts. The relatively poor accuracy in classifying cases in the intermediate time-to-recurvature categories is attributed to the variability among the synoptic fields that precede recurvature.

The overall accuracy (78% correct) in identifying storm motion during the 72-h forecast period can be improved if classifications are only into two groups (recurver versus straight), rather than into the nine 12-h time-to-recurvature groups plus PRNR. Similarly, skill can be improved if three groups defined as imminent (0–24 h), medium (36–72 h), and small (>72 h) likelihood of recurvature are adopted. Consequently, the number and composition of the classification groups must be a trade-off between the forecaster's need to specify a precise time of recurvature and the diminishing accuracy as more time precision is attempted in the forecast model.

The EOF coefficients based on the 250-mb vorticity fields have slightly better time-to-recurvature forecast accuracy than at 400 or 700 mb. The coefficients for this pressure level are statistically the most distinct among the time-to-recurvature groups and the 250-mb eigenvectors represent more variance in the vorticity fields than those for the other two pressure levels. The availability of satellite cloud-drift winds and aircraft reports may provide sufficiently accurate upper-tropospheric vorticity fields for operational application.

The results from these feasibility tests indicate the usefulness of an EOF representation of synoptic vorticity at one pressure level. Better accuracy may be achieved if the EOF coefficients for more than one pressure level are used, or if this EOF representation of the synoptic fields is combined with other factors such as persistence and climatology. Other analysis methods, such as multiple linear regression, that better exploit the time trends in continuous data of this type should also be tested. As more data become available, independent testing and stratification of the sample will be possible.

One problem with this initial investigation may be that it is assumed that only one set of vorticity patterns leads to recurvature. In fact, several distinct paths may be defined by the time-dependent coefficients in multidimensional space. Such differences could be due to different forcing mechanisms associated with recurvature, or more simply due to the differences in the large-scale vorticity patterns with latitude. While these preliminary results in pinpointing the precise (12-h) time to recurvature are somewhat discouraging, the technique may be quite useful. Just the assurance that a storm has a high likelihood of recurvature could assist the forecaster in assessing the synoptic analyses and forecasts, evaluating the various objective guidance products, and thus producing more consistent and accurate track forecasts.

Acknowledgments. This research was sponsored by the Naval Postgraduate School Direct Research Fund.

Constructive comments by Hugh Willoughby improved the manuscript. Penny Jones carefully typed the manuscript.

REFERENCES

ATCR, 1984: Annual Tropical Cyclone Report Report Type, 196 pp. [Available from NAVOCEANCOMCEN/JTWC, COMNAVMARIANAS, Box 17, FPO San Francisco, CA 96630.]

Dixon, W. J., Ed., 1988: *BMPD Statistical Software Manual, Volume 1.* University of Los Angeles Press, 619 pp.

Dobos, P. H., and R. L. Elsberry, 1993: Forecasting tropical cyclone recurvature. Part I. Evaluation of existing methods. *Mon. Wea. Rev.*, **121,** 1273–1278.

Elsberry, R. L., 1987: Tropical cyclone motion. *A Global View of Tropical Cyclones,* Office of Naval Research, 91–131.

——, E. L. Weniger, and D. H. Meanor, 1988: A statistical tropical cyclone intensity forecast technique incorporating environmental wind and vertical wind shear information. *Mon. Wea. Rev.*, **116,** 2142–2154.

Gunzelman, M. J., 1991: Tropical cyclone motion due to environmental interactions represented by empirical orthogonal functions of the vorticity fields. M.S. thesis, Department of Meteorology, Naval Postgraduate School, 98 pp. [Available from Department of Meteorology, Naval Postgraduate School, Monterey, CA 93943.]

Harr, P. A., and R. L. Elsberry, 1991: Tropical cyclone track characteristics as a function of large-scale circulation anomalies. *Mon. Wea. Rev.*, **119,** 1448–1468.

Miller, R. J., T. L. Tsui, and A. J. Schrader, 1988: Climatology of North Pacific tropical cyclone tracks. Naval Environmental Prediction Research Facility, Tech. Rep. TR 88-10, 511 pp. [Available from Naval Research Laboratory, Naval Postgraduate School, Monterey, CA 93943.]

Peak, J. E., W. E. Wilson, R. L. Elsberry, and J. C.-L. Chan, 1986: Forecasting tropical cyclone motion using empirical orthogonal function representation of the environmental wind fields. *Mon. Wea. Rev.*, **114,** 2466–2477.

Preisendorfer, R. W., and T. P. Barnett, 1977: Significance tests for empirical orthogonal functions. Proc. Fifth Conf. on Probability and Statistics in Meteorology and Atmospheric Sciences, Las Vegas, Amer. Meteor. Soc., 169–172.

——, F. W. Zwiers, and T. P. Barnett, 1981: *Foundations of principal component selection rules. SIO Reference Series 81-4.* Scripps Institution of Oceanography, 192 pp.

Schott, T. B., J. C.-L. Chan, and R. L. Elsberry, 1987: Further applications of empirical orthogonal functions of wind fields for tropical cyclone motion studies. *Mon. Wea. Rev.*, **115,** 1225–1237.

Shaffer, A. R., and R. L. Elsberry, 1982: A statistical–climatological tropical cyclone track prediction technique using an EOF representation of the synoptic forcing. *Mon. Wea. Rev.*, **110,** 1945–1954.

U.S. Naval Weather Service, 1975: Numerical Environmental Products Manual, Report type, NAVAIR 50-1G-522, 155 pp. [Available from Fleet Numerical Oceanography Center, Naval Postgraduate School, Monterey, CA 93943.]